

Supporting Information

Molecular-Level Characterization of Carbonaceous Aerosols via Coupled Thermal-Optical Carbon Analysis and Ultra-High-Resolution FT-ICR Mass Spectrometry

Silvia Juliana Vesga-Martínez^{1,2}, Christopher Paul Rüger^{1,2,*}, Fabian Etscheidt^{1,3}, Martin Bauer¹,
Patrick Martens⁴, Anika Neumann^{2,5}, Hendryk Czech^{1,6}, Ralf Zimmermann^{1,2,6}

1 – Joint Mass Spectrometry Centre (JMSC) / Chair of Analytical Chemistry, University of Rostock, 18059
Rostock, Germany

2 – Department Life, Light & Matter (LLM), University of Rostock, 18059 Rostock, Germany

3 – Photonion GmbH, 19061 Schwerin, Germany

4 – University of the Bundeswehr Munich, Faculty of Mechanical Engineering, Institute of Chemistry and
Environmental Engineering, Werner-Heisenberg-Weg 39, 85577 Neubiberg, Germany

5 – Chair of Piston Machines and Internal Combustion Engines (LKV), Faculty of Mechanical Engineering
and Marine Technology, University of Rostock, 18059 Rostock, Germany

6 – Helmholtz Zentrum München GmbH, German Research Center for Environmental Health,
Neuherberg, Germany, Cooperation group “Comprehensive Molecular Analytics” (CMA), Joint Mass
Spectrometry Centre (JMSC), 85764 Munich, Germany

* – corresponding author: christopher.rueger@uni-rostock.de

Keywords: thermal-optical carbon analyzer, high-resolution mass spectrometry, carbonaceous aerosols,
atmospheric pressure photoionization, particulate matter

Table of Content

Table S1. Comprehensive Overview of Sample Types: Filter ID, Emission type, Emission source (with origin and specifications).

Table S2. Congruence coefficients for triplicate measurements of MGO 60 kW.

Table S3. Quantified carbon response for all fractions from the TOCA analysis across triplicate measurements.

Table S4. Arithmetic means parameters calculated from the elemental composition for each dataset.

Table S5. Compound classes and their respective n^0_c and b values from Li et al. obtained by least squares optimization using compounds from the NCI database.

Section S1. Calculation of molecular properties.

Figure S1. Photographic illustration of TOCA hyphenated to the APPI FT-ICR MS.

Figure S2. Blank filter subjected to TOCA APPI (+) FT-ICR MS analysis. a) Time-resolved thermal-optical carbon analyzer response (quantitative carbon signal based on the carbon dioxide NDIR measurement). b) Total Ion count (TIC). c) Average mass spectra (chemical noise).

Figure S3. Triplicate analysis of MGO 60 kW by TOCA positive-ion APPI FT-ICR MS. (a) Time-resolved thermal-optical carbon analyzer response (quantitative carbon signal based on the carbon dioxide NDIR measurement). (b) Total ion count (TIC) zoomed-in OC2 fraction and fraction average mass spectra. (c) Bar plot of the relative summed intensity for major compound classes identified in the triplicates. (d) Venn and upset diagram illustrating the overlap of compounds across the triplicates.

Figure S4. Stacked plot of thermal-optical carbon analyzer response according to the desorption steps for triplicates of MGO 60 kW aerosol.

Figure S5. Total ion count (TIC) comparison for the TOF (yellow) and ICR (purple) platforms, overlapped and normalized for the engine samples. (a) HS-HFO 2.4 w-%S 60 kW, (b) ULS-HFO 0.06 w-%S 60 kW, (c) Marine Gas Oil (MGO) 60 kW.

Figure S6. Engine combustion aerosols analyzed by TOCA APPI (+) FT-ICR MS) Time-resolved thermal-optical carbon analyzer response (quantitative carbon signal based on the carbon dioxide NDIR measurement) (left), Total Ion Count (TIC) (middle) and entire run average mass spectra

(right) for: HS-HFO 2.4 w-%S 60 kW, ULS-HFO 0.06 w-%S 60 kW, and Marine Gas Oil (MGO) 60 kW.

Figure S7. Mass spectra and pie charts color-coded by compound class for the OC1-4 fractions of engine aerosol samples. Pie chart size is proportional to intensity. Samples include: HS-HFO 2.4 w-%S at 60 kW, ULS-HFO 0.06 w-%S at 60 kW, and Marine Gas Oil (MGO) at 60 kW.

Figure S8. Residential wood combustion analyzed by TOCA APPI (+) FT-ICR MS: a) Time-resolved thermal optical carbon analyzer response (quantitative carbon signal based on the carbon dioxide NDIR measurement), b) TIC, c) Sum-up mass spectra, and d) mass spectra with pie charts color-coded by compound class for OC1-4 fractions.

Figure S9. Seasonal ambient aerosols: a) Time-resolved thermal-optical carbon analyzer response (quantitative carbon signal based on the carbon dioxide NDIR measurement). b) Total Ion Count (TIC) and average mass spectra overlapped for Autumn and spring samples.

Figure S10. Aromaticity (DBE) versus carbon number (#C) for OC1-3 fractions of: a) HS-HFO 60 kW, b) ULS-HFO 60 kW c) Marine gas oil (MGO) 60 kW. Color-coded for compound classes and size defined by signal intensity. Intensity normalized to each fraction.

Figure S11. Aromaticity (DBE) versus carbon number (#C) for OC1-4 fractions of RWC sample. Color-coded for compound classes and size defined by signal intensity. Intensity normalized to each fraction.

Figure S12. Double bond equivalent (DBE) versus carbon number for all compound classes in OC fractions from Autumn (top) and Spring (bottom) ambient samples. Compound classes are represented by color, with relative intensity indicated by dot size. Intensity is normalized to 2×10^8 a.u. The pie chart illustrates the percentage distribution of each compound class in each fraction.

Figure S13. The Van Krevelen diagram of O/C versus H/C ratio by OC fractions indicated by color for: a) engine fuel combustion: HS-HFO 60 kW (left top), ULS-HFO 60 kW (left middle) and Marine gas oil (MGO) 60 kW (left bottom), b) Residential wood combustion (RWC), c) Autumn (right middle) and spring (right bottom) ambient samples. Color coding differentiating each fraction and dot size reflecting the relative intensity within each fraction. The intensity-weighted average H/C and O/C ratios for each fraction are represented by an \diamond symbol, color-coded to match the respective fraction.

Table S1. Comprehensive Overview of Sample Types: Filter ID, Emission type, Emission source (with origin and specifications).

Filter sample	Emission type	Source	Additional information
MGO	POA	shipping fuel	Engine load – 60 kW
Ultra-low-sulfur HFO (0.06 w-%S) (ULS-HFO)	POA	shipping fuel	Engine load – 60 kW
High-sulfur HFO (2.4 w-%S) (HS-HFO)	POA	shipping fuel	Engine load – 60 kW
Residential wood combustion (RWC)	Wood POA	Biomass burning	Beech wood
Beijing -Autumn	Ambient	Particulate matter	PM ₄ Seasonal: Autumn
Beijing -Spring	Ambient	Particulate matter	PM ₄ Seasonal: Spring

Table S2. Congruence coefficients for triplicate measurements of MGO 60 kW.

coefficient of congruence		Replicate 01	Replicate 02	Replicate 03
Replicate	01	1	0.986	0.985
	02	0.986	1	0.9812
	03	0.984	0.982	1

Table S3. Quantified carbon response for all fractions from the TOCA analysis across triplicate measurements.

Fraction	OC1	OC2	OC3	OC4	TOC	EC1	EC2	EC3	TEC
Replicate 01	0.0	13.48	10.66	3.27	27.41	0.32	61.39	8.43	70.14
Replicate 02	0.0	12.45	11.50	3.29	27.24	1.46	59.73	11.85	72.99
Replicate 03	0.0	11.54	11.88	3.64	27.06	0.82	58.04	6.30	65.15

Table S4. Arithmetic means parameters calculated from the elemental composition for each dataset.

Sample	Compounds	H/C	O/C	N/C	S/C	O/N	DBE	log(C*)	OS _c
HS-HFO	701	1.26	0.06	-	0.06	-	7.78	1.87	-1.24
ULS-HFO	948	1.02	0.09	0.06	0.06	1.70	9.62	2.06	-0.37
MGO	682	1.45	0.07	-	-	-	6.23	1.27	-1.40
RWC	1356	0.65	0.09	0.06	-	1.26	14.49	1.22	-0.55

Table S5. Compound classes and their respective n_c^0 and b values from Li et al.¹ obtained by least squares optimization using compounds from the NCI database.²

Compound class	n_c^0	b_c	b_o	b_{co}	b_n	b_s
CH	23.8	0.4861				
CHO	22.66	0.4481	1.656	-0.7790		
CHN	24.59	0.4066			0.9619	
CHNO	24.13	0.3667	0.7732	-0.07790	1.114	
CHOS	24.06	0.3637	1.327	-0.3988		0.7579

Section S1. Calculation of molecular properties.

Formulae applied for the calculation of double bond equivalents (DBE), aromaticity index (AI, modified for high oxygen content), average carbon oxidation state (OS_c), saturation mass concentration (C_0 , Table S5). Calculations are based on the assigned neutral sum formulae $C_cH_hN_nO_oS_s$.^{2,3,1}

$$DBE = c - \frac{h}{2} + \frac{n}{2} + 1 \quad (1)$$

$$AI_{mod} = \frac{1 + c - 0.5o - s - 0.5h}{c - 0.5o - s - n} \quad (2)$$

$AI_{mod} > 0.5$ indicates aromatic structures and $AI_{mod} > 0.67$ indicates condensed aromatic structures.

$$OS_c = 2\frac{o}{c} - \frac{h}{c} \quad (3)$$

$$\log_{10}C_0 = (n_c^0 - c)b_c - ob_o - 2\frac{co}{c+o}b_{co} - nb_n - sb_s \quad (4)$$

Organic aerosol compounds can be classified into five groups, based on their saturation mass concentration (C_0): volatile organic compounds (VOC; $C_0 > 3 \times 10^6 \mu\text{g m}^{-3}$), intermediate volatility OC (IVOC; $300 < C_0 < 3 \times 10^6 \mu\text{g m}^{-3}$), semi volatile OC (SVOC; $0.3 < C_0 < 300 \mu\text{g m}^{-3}$), low-volatile OC (LVOC; $3 \times 10^{-4} < C_0 < 0.3 \mu\text{g m}^{-3}$), and extremely low-volatile (ELVOC; $C_0 < 3 \times 10^{-4} \mu\text{g m}^{-3}$).^{4,1}

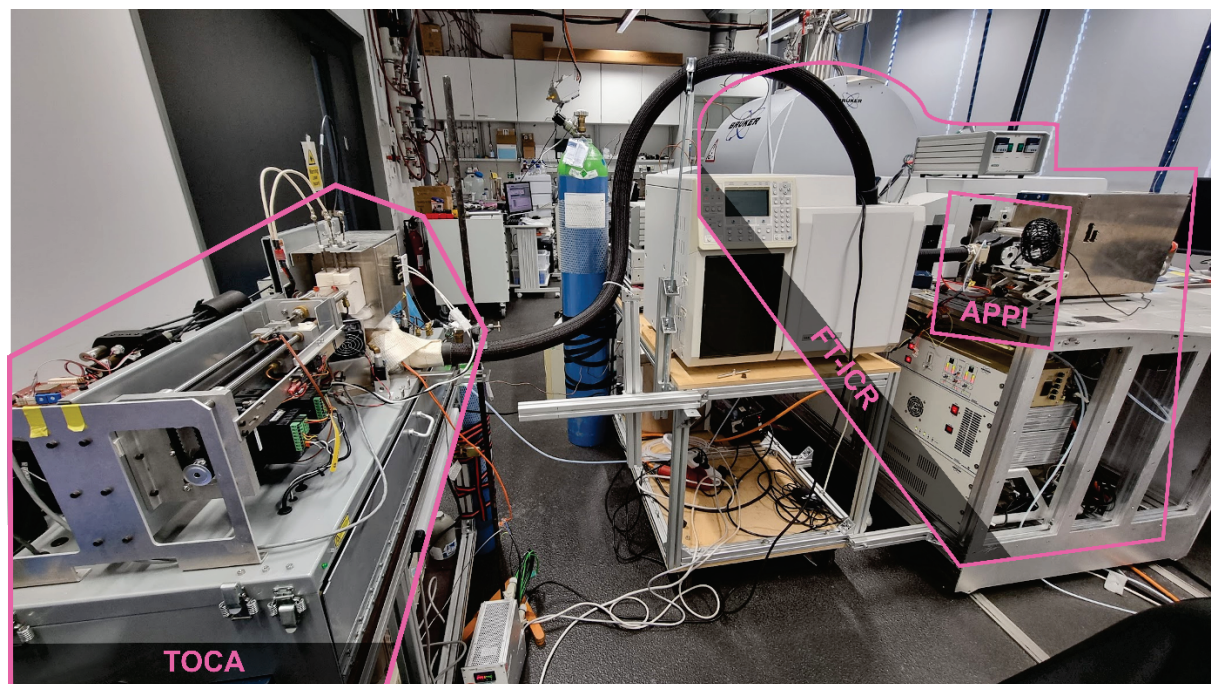


Figure S1. Photographic illustration of TOCA hyphenated to the APPI FT-ICR MS.

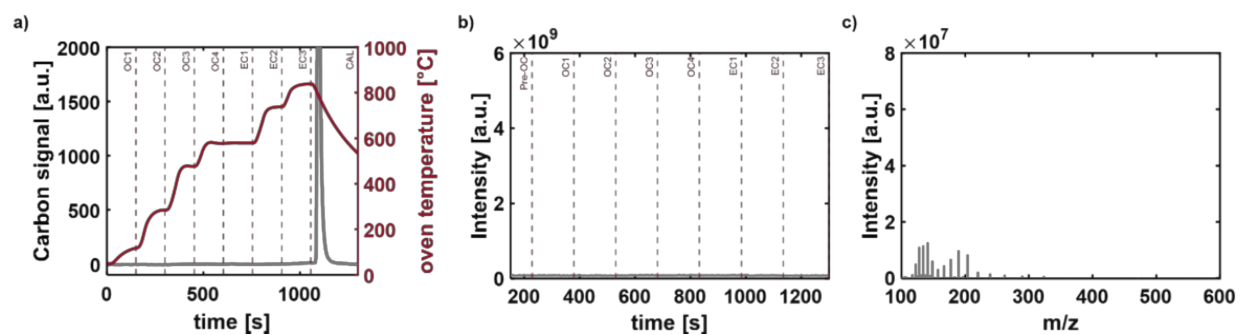


Figure S2. Blank filter subjected to TOCA APPI (+) FT-ICR MS analysis. a) Time-resolved thermal-optical carbon analyzer response (quantitative carbon signal based on the carbon dioxide NDIR measurement). b) Total Ion count (TIC). c) Average mass spectra (chemical noise).

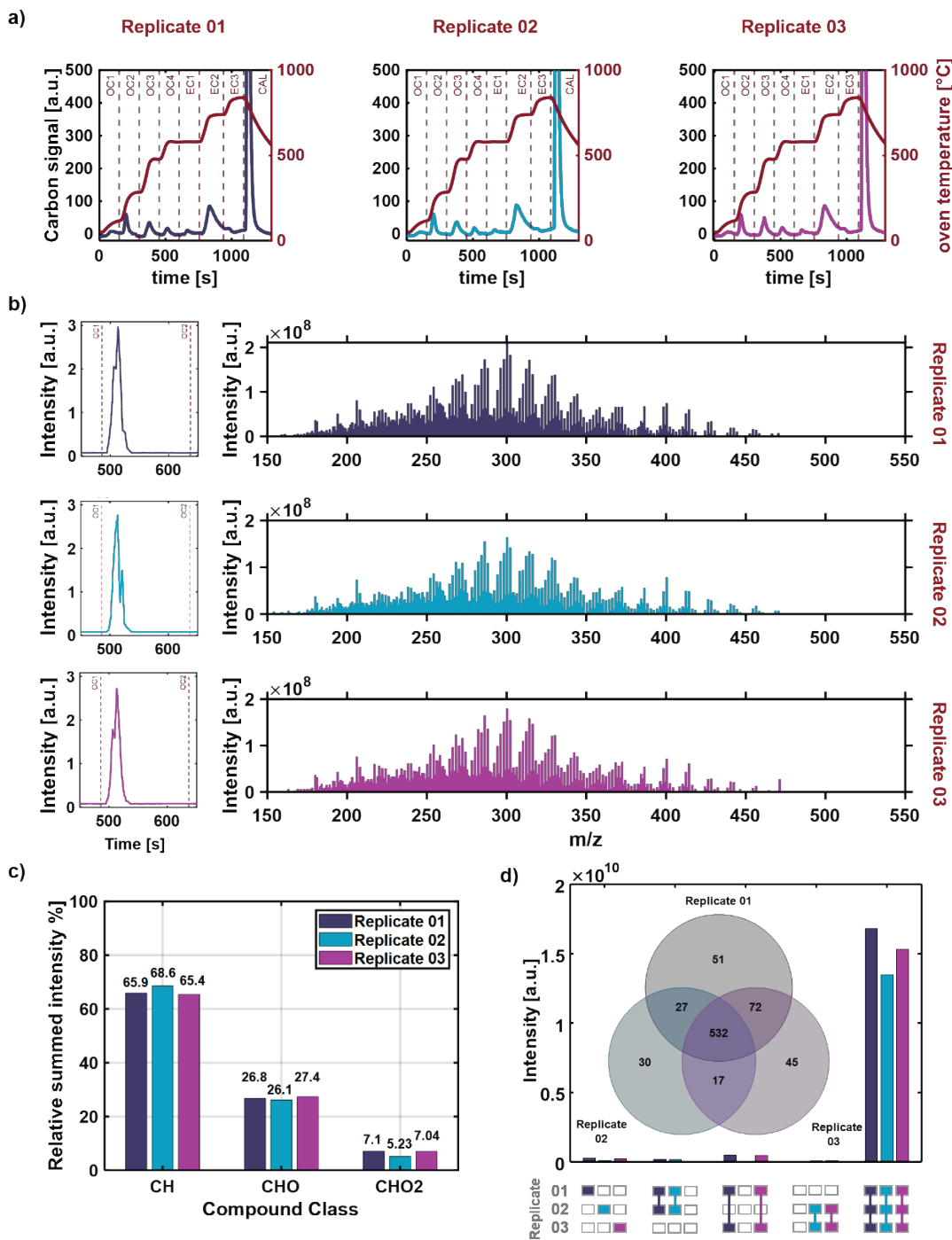


Figure S3. Triplicate analysis of MGO 60 kW by TOCA positive-ion APPI FT-ICR MS. (a) Time-resolved thermal-optical carbon analyzer response (quantitative carbon signal based on the carbon dioxide NDIR measurement). (b) Total ion count (TIC) zoomed-in OC2 fraction and fraction average mass spectra. (c) Bar plot of the relative summed intensity for major compound classes identified in the triplicates. (d) Venn and upset diagram illustrating the overlap of compounds across the triplicates.

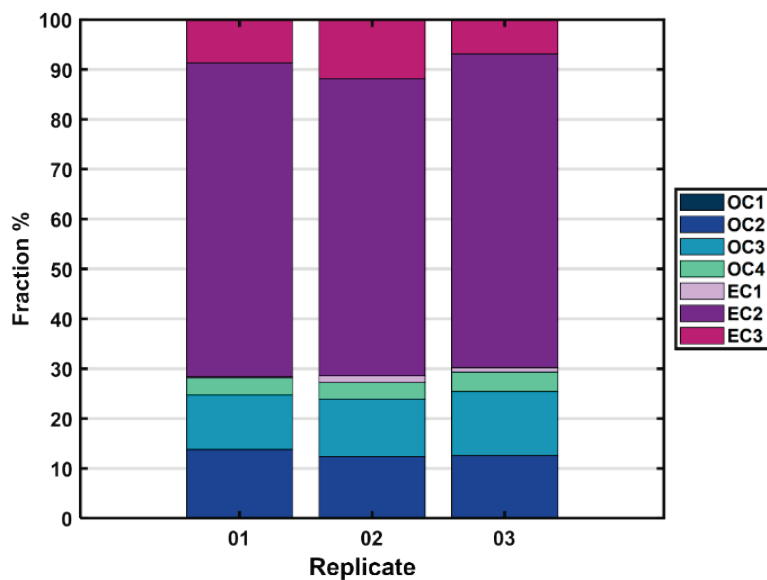


Figure S4. Stacked plot of thermal-optical carbon analyzer response according to the desorption steps for triplicates of MGO 60 kW aerosol.

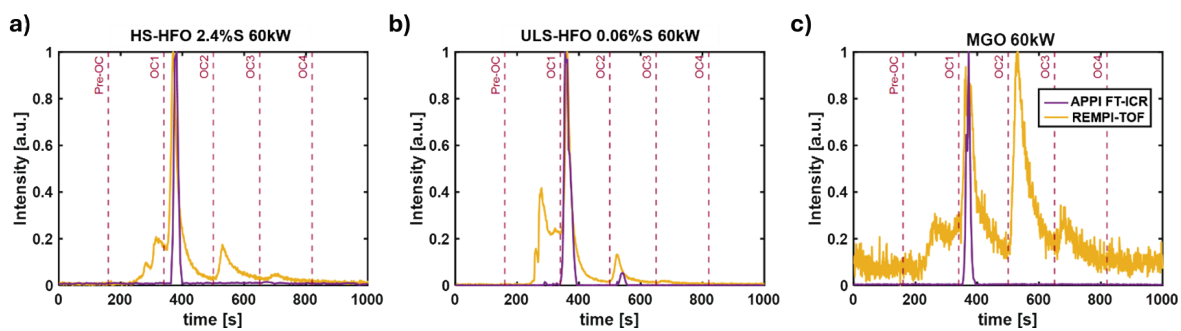


Figure S5. Total ion count (TIC) comparison for the TOF (yellow) and ICR (purple) platforms, overlapped and normalized for the engine samples. (a) HS-HFO 2.4%S 60 kW, (b) ULS-HFO w-0.06%S 60 kW, (c) Marine Gas Oil (MGO) 60 kW.

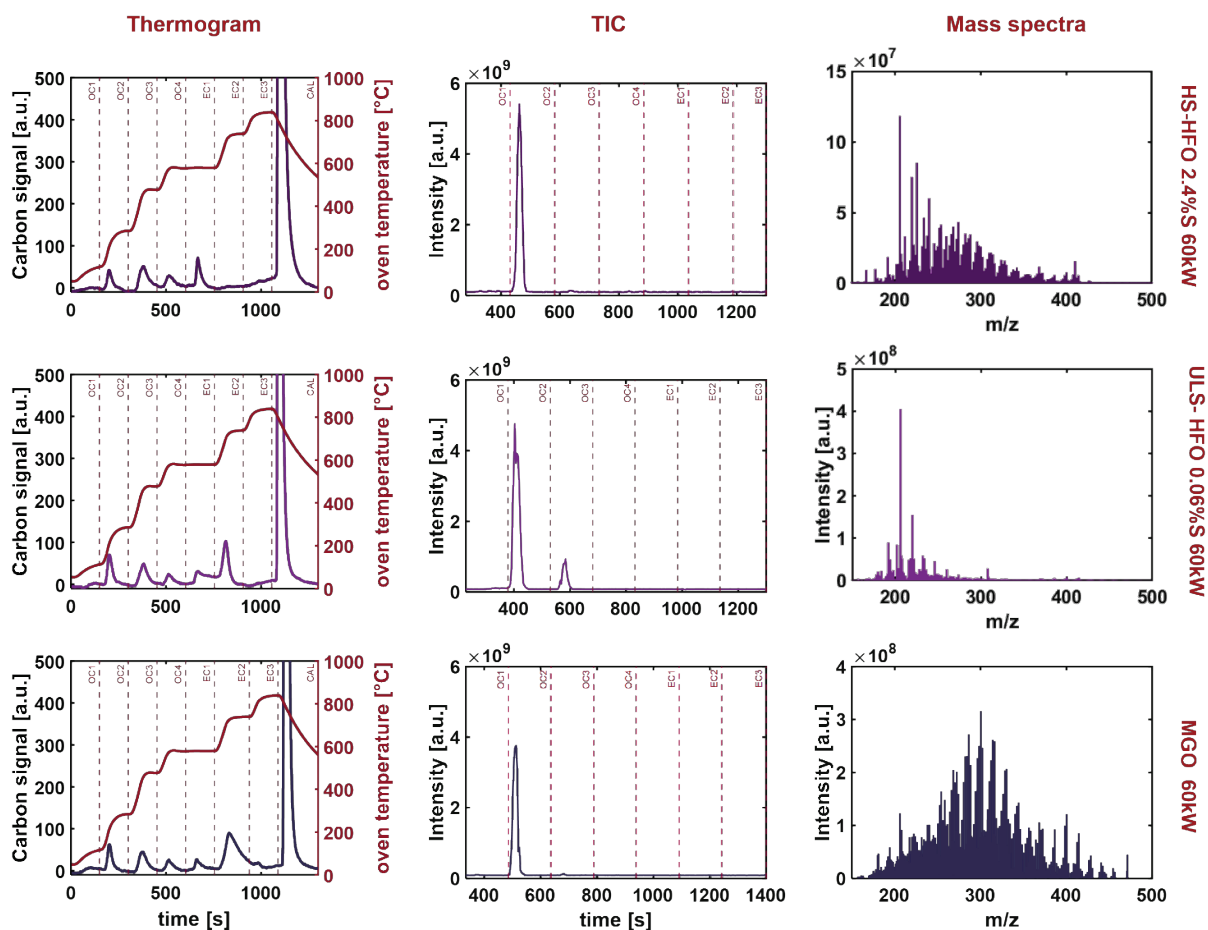


Figure S6. Engine combustion aerosols analyzed by TOCA APPI (+) FT-ICR MS) Time-resolved thermal-optical carbon analyzer response (quantitative carbon signal based on the carbon dioxide NDIR measurement) (left), Total Ion Count (TIC) (middle) and entire run average mass spectra (right) for: HS-HFO 2.4%S 60 kW, ULS-HFO 0.06%S 60 kW, and Marine Gas Oil (MGO) 60 kW.

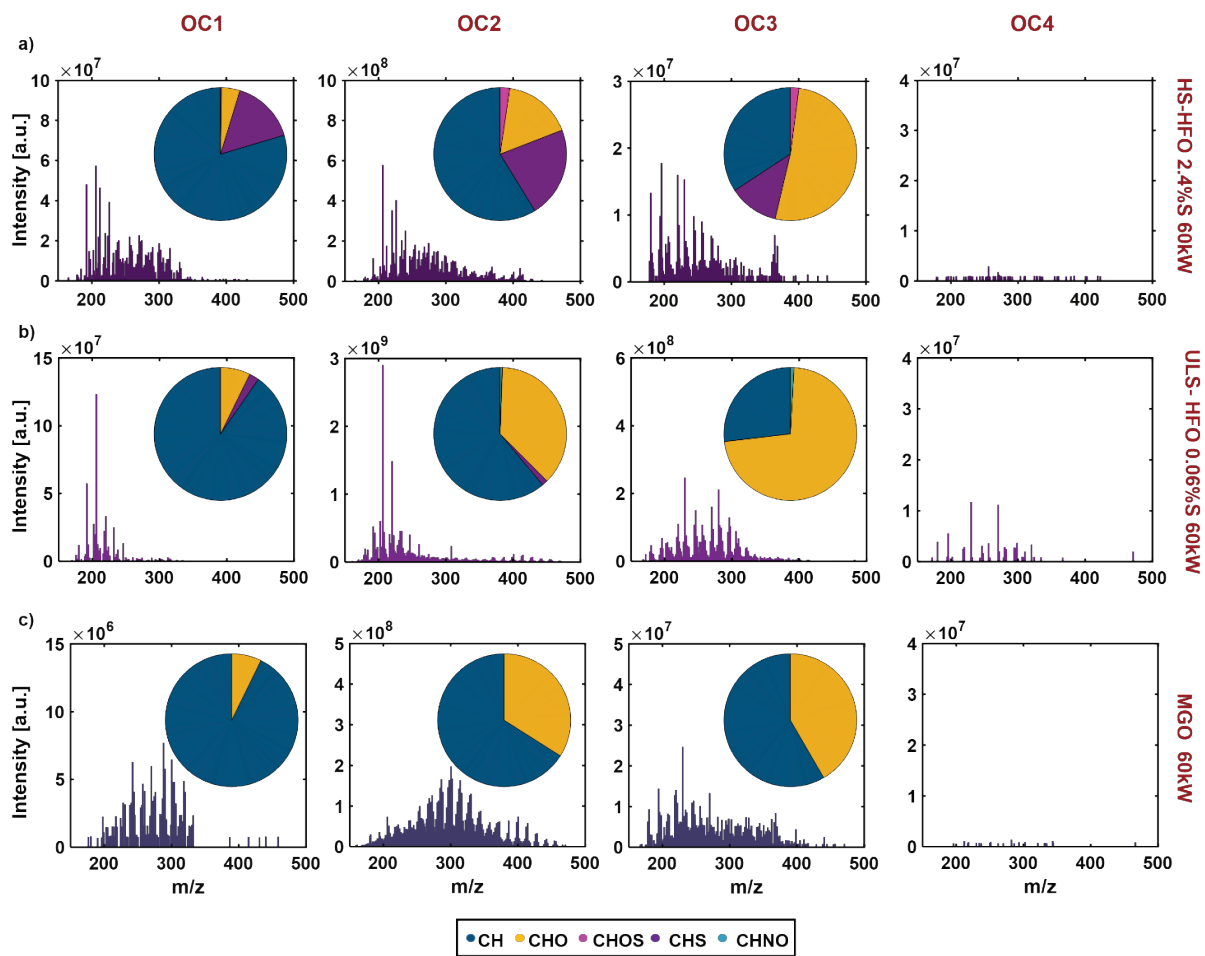


Figure S7. Mass spectra and pie charts color-coded by compound class for the OC1-4 fractions of engine aerosol samples. Pie chart size is proportional to intensity. Samples include: HS-HFO 2.4 w-%S at 60 kW, ULS-HFO 0.06 w-%S at 60 kW, and Marine Gas Oil (MGO) at 60 kW.

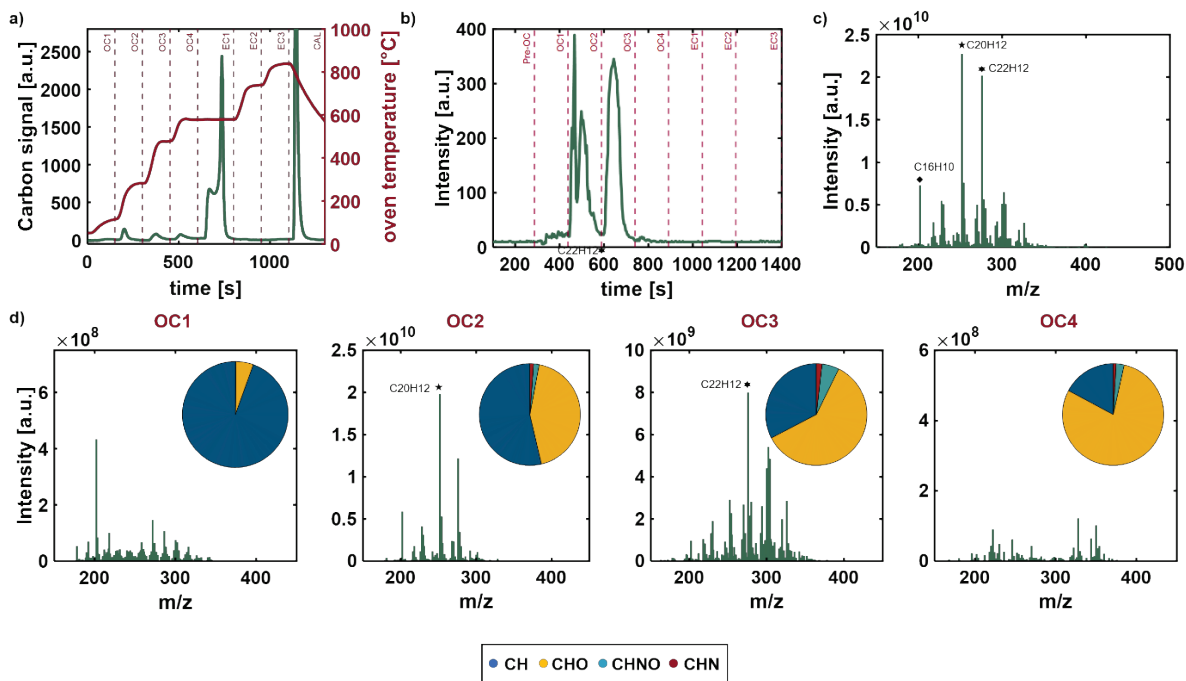


Figure S8. Residential wood combustion analyzed by TOCA APPI (+) FT-ICR MS: a) Time-resolved thermal optical carbon analyzer response (quantitative carbon signal based on the carbon dioxide NDIR measurement), b) TIC, c) Sum-up mass spectra, and d) mass spectra with pie charts color-coded by compound class for OC1-4 fractions.

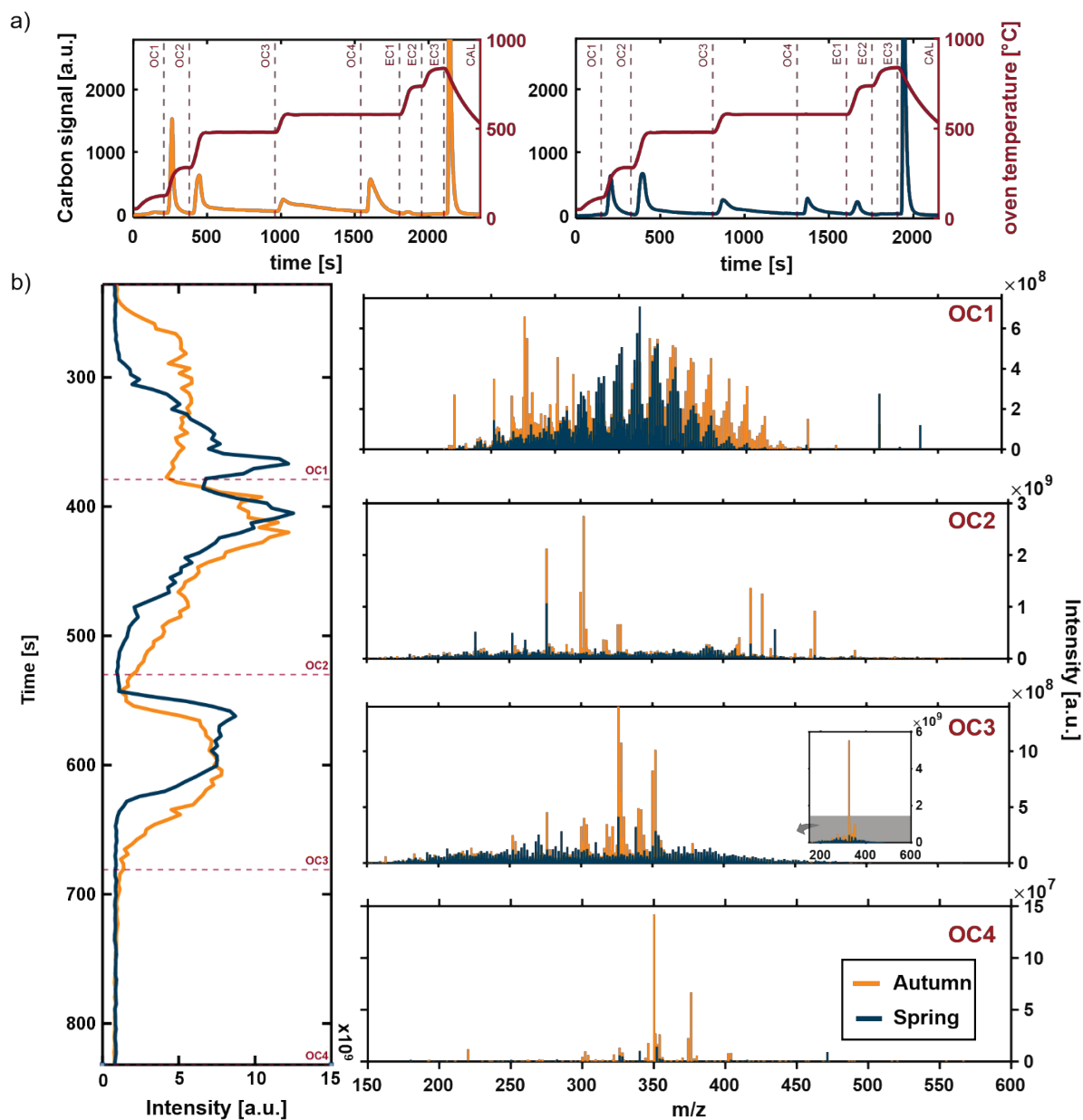


Figure S9. Seasonal ambient aerosols: a) Time-resolved thermal-optical carbon analyzer response (quantitative carbon signal based on the carbon dioxide NDIR measurement). b) Total Ion Count (TIC) and average mass spectra overlapped for Autumn and spring samples.

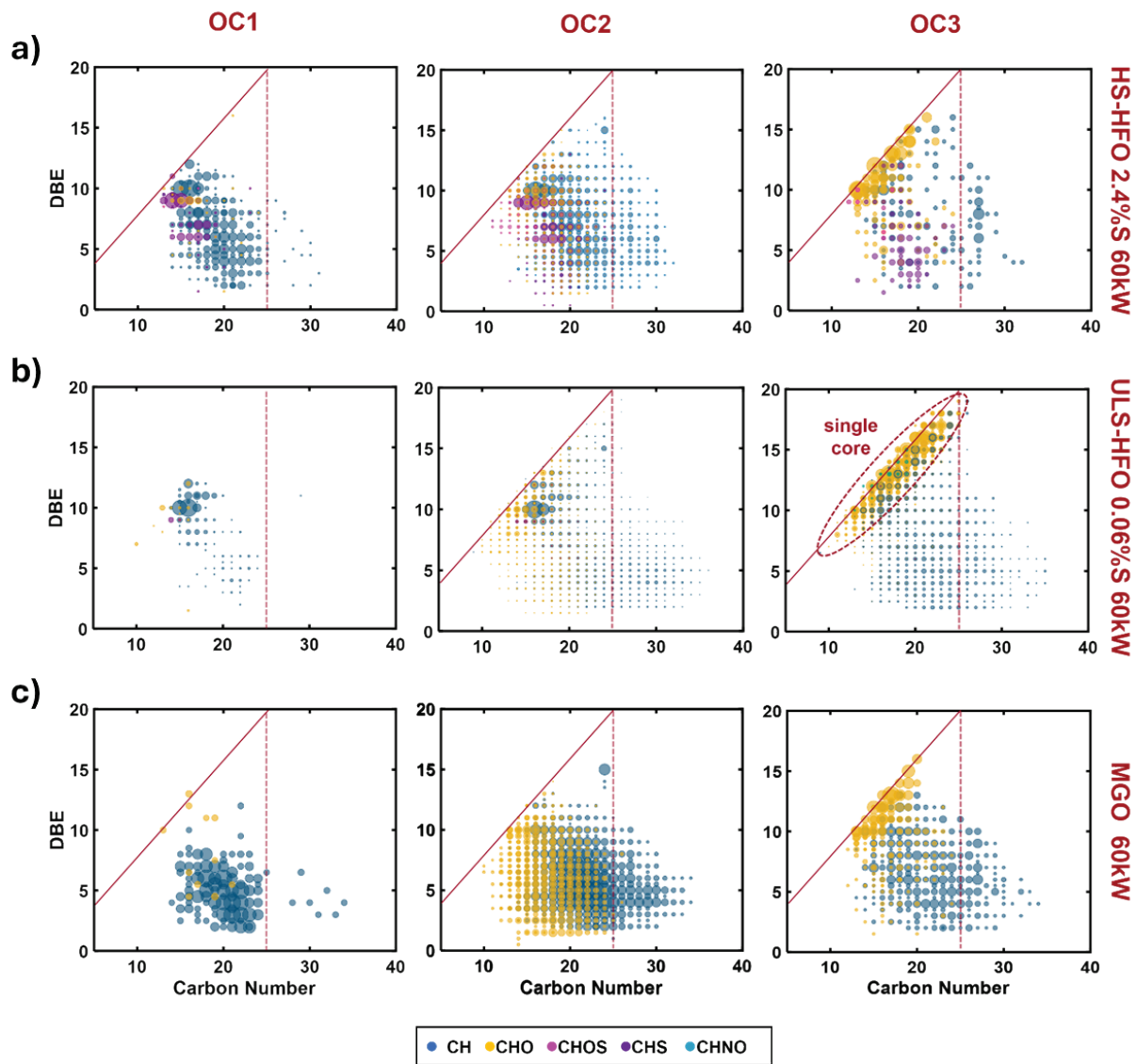


Figure S10. Aromaticity (DBE) versus carbon number (#C) for OC1-3 fractions of: a) HS-HFO 60 kW, b) ULS-HFO 60 kW c) Marine gas oil (MGO) 60 kW. Color-coded for compound classes and size defined by signal intensity. Intensity normalized to each fraction.

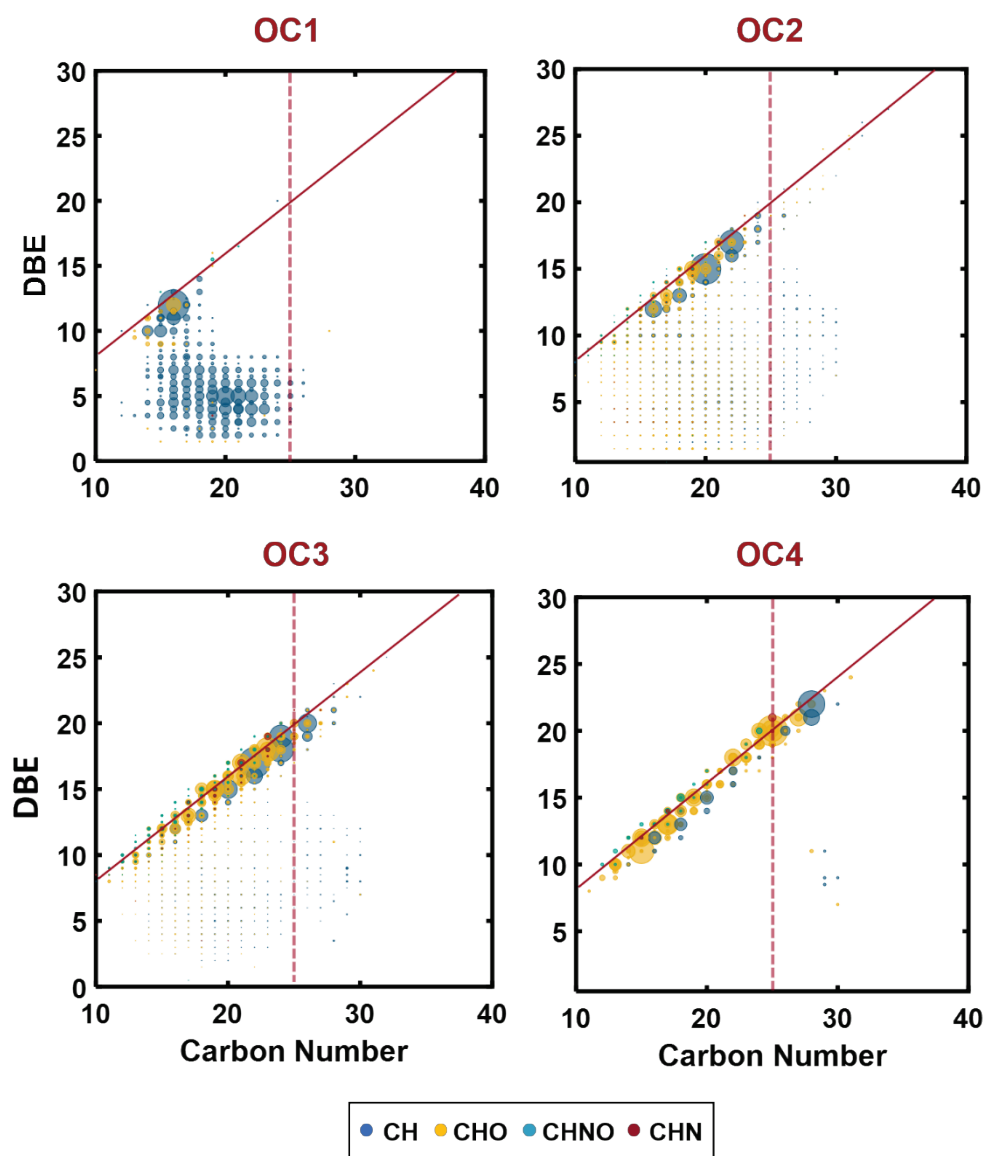


Figure S11. Aromaticity (DBE) versus carbon number (#C) for OC1-4 fractions of RWC sample. Color-coded for compound classes and size defined by signal intensity. Intensity normalized to each fraction.

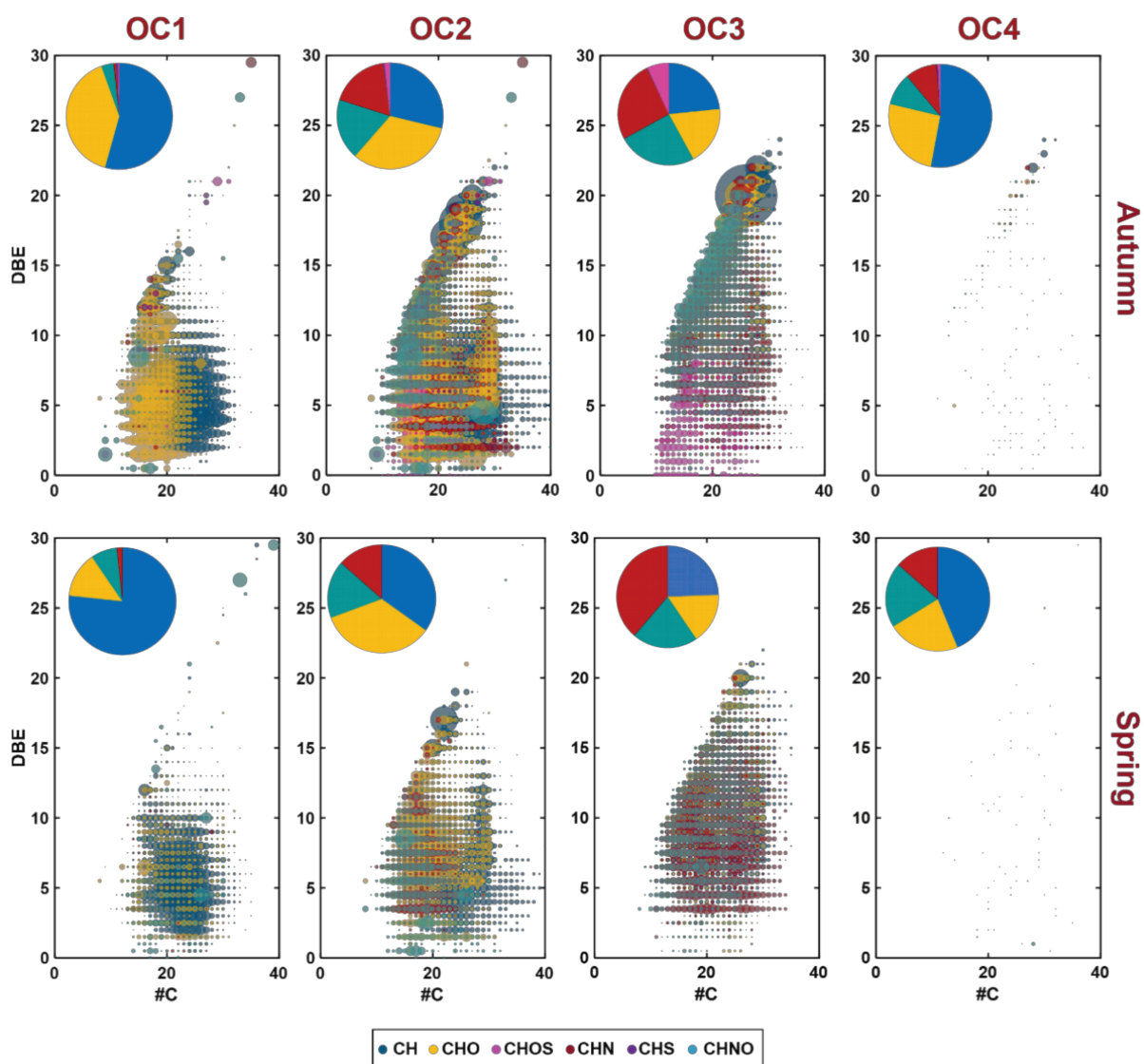


Figure S12. Double bond equivalent (DBE) versus carbon number for all compound classes in OC fractions from Autumn (top) and Spring (bottom) ambient samples. Compound classes are represented by color, with relative intensity indicated by dot size. Intensity is normalized to 2×10^8 a.u. The pie chart illustrates the percentage distribution of each compound class in each fraction.

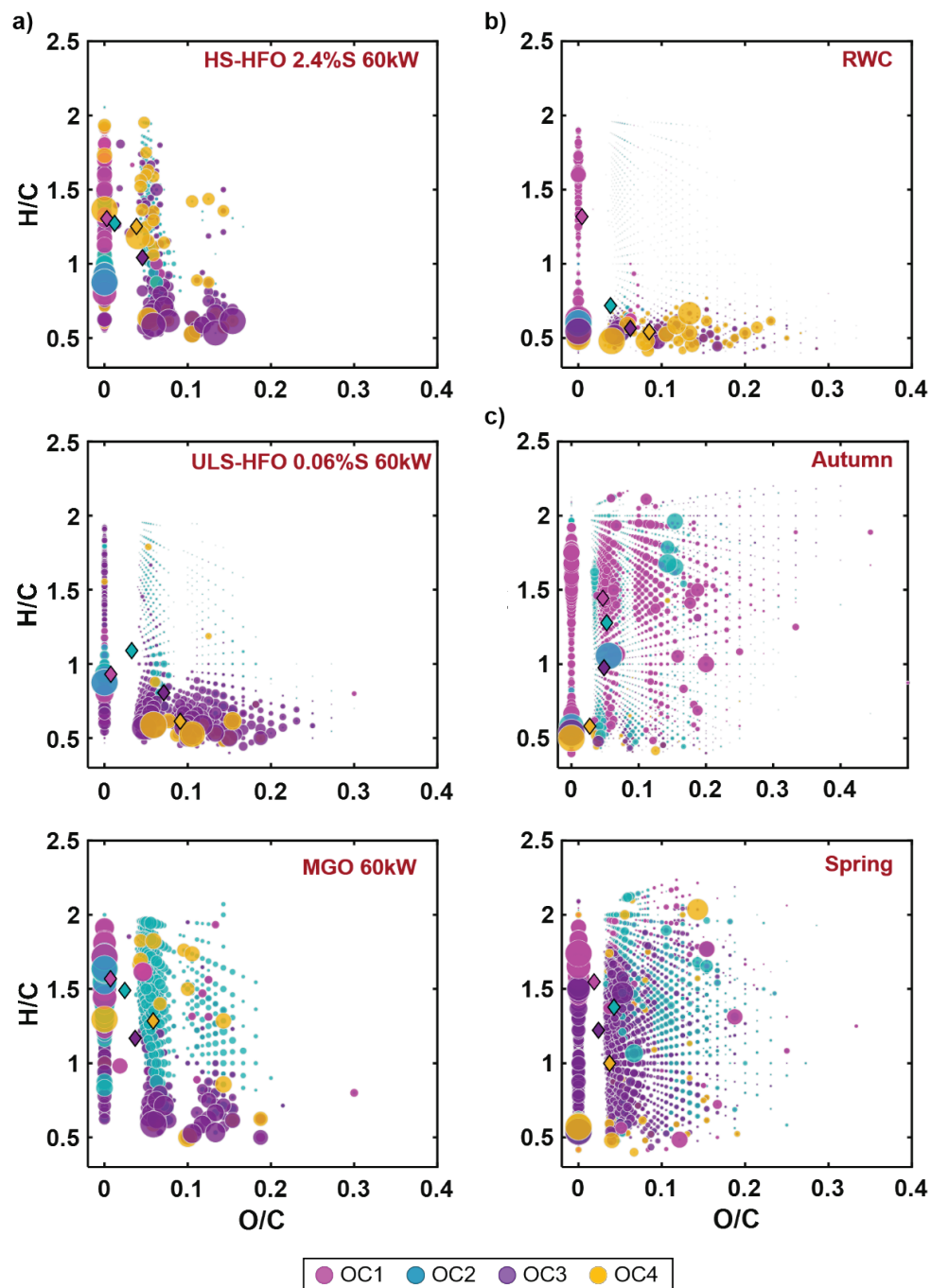


Figure S13. The Van Krevelen diagram of O/C versus H/C ratio by OC fractions indicated by color for: a) engine fuel combustion: HS-HFO 60 kW (left top), ULS-HFO 60 kW (left middle) and Marine gas oil (MGO) 60 kW (left bottom), b) Residential wood combustion (RWC), c) Autumn (right middle) and spring (right bottom) ambient samples. Color coding differentiating each fraction and dot size reflecting the relative intensity within each fraction. The intensity-weighted average H/C and O/C ratios for each fraction are represented by an \diamond symbol, color-coded to match the respective fraction.

References

- (1) Li, Y.; Pöschl, U.; Shiraiwa, M. Molecular corridors and parameterizations of volatility in the chemical evolution of organic aerosols. *Atmos. Chem. Phys.* **2016**, *16*, 3327–3344, DOI: 10.5194/acp-16-3327-2016.
- (2) Koch, B. P.; Dittmar, T. From mass to structure: an aromaticity index for high-resolution mass data of natural organic matter. *Rapid Comm Mass Spectrometry* **2006**, *20*, 926–932, DOI: 10.1002/rcm.2386.
- (3) Kroll, J. H.; Donahue, N. M.; Jimenez, J. L.; Kessler, S. H.; Canagaratna, M. R.; Wilson, K. R.; Altieri, K. E.; Mazzoleni, L. R.; Wozniak, A. S.; Bluhm, H.; Mysak, E. R.; Smith, J. D.; Kolb, C. E.; Worsnop, D. R. Carbon oxidation state as a metric for describing the chemistry of atmospheric organic aerosol. *Nature chemistry* **2011**, *3*, 133–139, DOI: 10.1038/nchem.948.
- (4) Donahue, N. M.; Epstein, S. A.; Pandis, S. N.; Robinson, A. L. A two-dimensional volatility basis set: 1. organic-aerosol mixing thermodynamics. *Atmos. Chem. Phys.* **2011**, *11*, 3303–3318, DOI: 10.5194/acp-11-3303-2011.